

Analytical Models of the Performance of C-V2X Mode 4 Vehicular Communications

Manuel Gonzalez-Martin, Miguel Sepulcre, Rafael Molina-Masegosa, Javier Gozalvez

Abstract— The C-V2X or LTE-V standard has been designed to support V2X (Vehicle to Everything) communications. The standard is an evolution of LTE, and it has been published by the 3GPP in Release 14. This new standard introduces the C-V2X or LTE-V Mode 4 that is specifically designed for V2V communications. In Mode 4, vehicles autonomously select and manage their radio resources without any cellular infrastructure support. Mode 4 is highly relevant since V2V safety applications cannot depend on the availability of infrastructure-based cellular coverage. This paper presents a set of novel analytical models of the communication performance of C-V2X or LTE-V Mode 4. In particular, the paper presents analytical models for the average PDR (Packet Delivery Ratio) as a function of the distance between transmitter and receiver, and for the four different types of transmission errors that can be encountered in C-V2X or LTE-V Mode 4. The models are validated in this study for a wide range of transmission parameters and traffic densities. To this aim, this study compares the results obtained with the analytical models to those obtained with a C-V2X or LTE-V Mode 4 simulator implemented by the authors over the Veins simulation platform. To the authors' knowledge, the models presented in this paper are the first to analytically model the communication performance of C-V2X or LTE-V Mode 4.

Index Terms—C-V2X, LTE-V, Mode 4, cellular V2X, LTE-V2X, V2V, communication, analytical, model, connected vehicles.

I. INTRODUCTION

The Third Generation Partnership Project (3GPP) published in Release 14 an evolution of the LTE standard to support V2X (Vehicle to Everything) communications. This evolution is commonly referred to as C-V2X, Cellular V2X, LTE-V, LTE-V2X or LTE-V2V [1]. C-V2X is considered an alternative to IEEE 802.11p since it supports direct communication between vehicles using the PC5 interface (also known as V2X sidelink communications). Release 14 introduces two new communication modes (Mode 3 and Mode 4) specifically designed for V2V (Vehicle to Vehicle) communications. In Mode 3, the cellular network selects and manages the radio resources used by vehicles for their direct V2V communications. In Mode 4, vehicles autonomously select and manage the resources without any cellular

infrastructure support. To this aim, Mode 4 defines a sensing-based Semi-Persistent Scheduling (SPS) scheme for vehicles to autonomously select their radio resources. Mode 4 is highly relevant since V2V safety applications cannot depend on the availability of infrastructure-based cellular coverage.

Recent studies have analyzed the performance of C-V2X Mode 4 and compared it to that achieved with IEEE 802.11p standards such as DSRC or ITS-G5 [2][3]. These studies are based on network simulations, and to the authors' knowledge there are no analytical models of the C-V2X Mode 4 communication performance in the literature. Existing and recent C-V2X analytical models focus on C-V2X Mode 3 where the radio resources are managed and assigned by the infrastructure. For example, [4] proposes analytical models using combined Markov chains to evaluate the performance of different scheduling schemes in C-V2X. [5] analytically models C-V2X considering that resources are managed and assigned by the infrastructure (i.e. Mode 3), and compares its scalability to that of IEEE 802.11p. The authors utilize the model proposed in [6] to analyze the beaconing resource occupation. Prior to [4] and [5], other studies have reported analytical models for V2I (Vehicle to Infrastructure) communications using LTE. For example, [7] proposes a M/M/m queuing model to evaluate the probability that a vehicle finds all channels busy, and to derive the expected waiting times. An analytical framework is proposed in [8] to compare IEEE 802.11p and LTE in terms of the probability to deliver a packet before a deadline. This study considers that vehicles transmit their packets in an uplink channel to the LTE base station, and the base station retransmits the relevant packets to each vehicle over a downlink channel.

Analytical models are an important evaluation tool to provide insights of the performance under a wide range of parameters and conditions. These analyses can then be complemented by more comprehensive, but also more computationally expensive, network simulations. In this context, this paper presents and validates the first analytical models of the communication performance of C-V2X Mode 4. The models provide the average PDR (Packet Delivery Ratio) as a function of the distance between transmitter and receiver. In addition, the models quantify the four different types of packet errors that affect C-V2X Mode 4 [9]: errors due to half-duplex transmissions, errors due to a received signal power below the sensing power threshold, errors due to propagation effects, and errors due to packet collisions. The accuracy of the proposed model is validated by comparing its results to

Manuscript received July 2018. This work was supported in part by the Spanish Ministry of Economy and Competitiveness and FEDER funds under the projects TEC2014-57146-R and TEC2017-88612-R, and research grant PEJ-2014-A33622.

Manuel Gonzalez-Martin, Miguel Sepulcre, Rafael Molina-Masegosa and Javier Gozalvez are with the UWICORE Laboratory, Universidad Miguel Hernandez de Elche (UMH), Spain. E-mail: manuel.gonzalez@umh.es, msepulcre@umh.es, rafael.molinam@umh.es, j.gozalvez@umh.es.

those obtained using a comprehensive C-V2X Mode 4 network simulator developed by the authors in Veins and presented in [9]. The model is validated for a wide range of transmission parameters and traffic densities. In particular, the model has been validated for several transmission power levels, Modulation and Coding Schemes (MCS) and sub-channelizations, and packet transmission frequencies.

II. C-V2X MODE 4

A. Physical layer

C-V2X utilizes SC-FDMA and supports 10 and 20MHz channels. Each channel is divided into sub-frames, Resource Blocks (RBs), and sub-channels. Sub-frames are 1ms long (like the Transmission Time Interval). A RB is the smallest unit of frequency resources that can be allocated to a LTE user. It is 180kHz wide in frequency (12 sub-carriers of 15kHz). C-V2X defines sub-channels as a group of RBs in the same sub-frame. The number of RBs per sub-channel can vary. Sub-channels are used to transmit data and control information, where the control information (referred to as Sidelink Control Information or SCI) occupies 2RBs. The data is transmitted in Transport Blocks (TBs). A TB contains a full packet to be transmitted, e.g. a packet or a CAM (Cooperative Awareness Messages)/BSM (Basic Safety Messages). TBs can be transmitted using QPSK or 16-QAM and turbo coding. The maximum transmit power is 23dBm, and the standard requires a sensitivity power level at the receiver of -90.4dBm [10]. Fig. 1 (left part) illustrates the C-V2X sub-channelization when the available bandwidth is divided in 4 sub-channels and the control information is adjacent to the data.

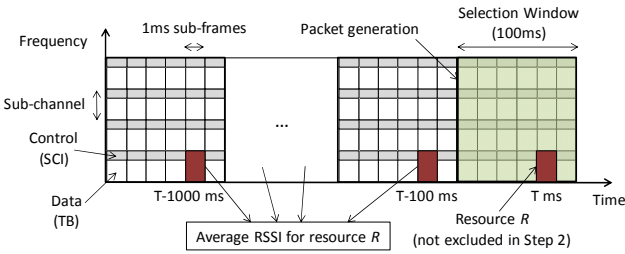


Fig. 1. C-V2X sub-channelization and average RSSI of a resource for $\lambda=10\text{Hz}$

B. Sensing-based Semi-Persistent Scheduling

In C-V2X Mode 4, vehicles autonomously select their resources using the sensing-based SPS scheme specified in Release 14 [11][12]. A vehicle reserves the selected resource(s) for a random number of consecutive packets that depends on the number of packets transmitted per second (λ) or inversely the packet transmission interval. For $\lambda=10\text{Hz}$, 20Hz and 50Hz, this random number is selected between 5 and 15, between 10 and 30, and between 25 and 75, respectively. When a vehicle needs to reserve new resources, it randomly selects a Reselection Counter. After each transmission, the Reselection Counter is decremented by one. When it is equal to zero, new resources must be selected and

reserved with probability $(1-p_{res})$ where $p_{res} \in [0,0.8]$ ¹. Each vehicle includes its packet transmission interval and the value of its Reselection Counter in its SCI. Vehicles use this information to estimate which resources are free when making their own reservation to reduce packet collisions. The process to reserve resources is organized in the following 3 steps.

Step 1. When a vehicle v_i needs to transmit a new packet and the Reselection Counter is zero, v_i has to reserve new resources within a Selection Window. The Selection Window is the time window between the time the packet has been generated (t_b) and the defined maximum latency (Fig. 1, right part). The maximum latency is 100ms for $\lambda=10\text{Hz}$, 50ms for $\lambda=20\text{Hz}$ and 20ms for $\lambda=50\text{Hz}$ [11]. Within the Selection Window, the vehicle identifies the resources that could be reserved. A resource is a group of adjacent sub-channels within the same sub-frame where the packet (SCI+TB) to be transmitted fits.

Step 2. Vehicle v_i then creates a list L_A of available resources it could reserve. This list includes all the resources previously identified in Step 1 except those that meet the following two conditions:

1) v_i has received in the last 1000 sub-frames an SCI from another vehicle indicating that it will utilize this resource in the Selection Window or any of its next *Reselection Counter* packets.

2) v_i measures an average Reference Signal Received Power (RSRP) over the resource higher than a given threshold.

Vehicle v_i also excludes all the resources of sub-frame f_i in the Selection Window if v_i was transmitting during any previous sub-frame f_j , where $j=i-100 \cdot k$ and $k \in \mathbb{N}$, $1 \leq k \leq 10$ for $\lambda=10\text{Hz}$ ².

After Step 2 is executed, L_A must contain at least 20% of all the resources in the Selection Window. If not, Step 2 is iteratively executed until the 20% target is met. In each iteration, the RSRP threshold is increased by 3dB.

Step 3. v_i creates a list of candidate resources L_C that includes the resources in L_A that experienced the lowest average RSSI (Received Signal Strength Indicator). The size of L_C must be equal to the 20% of all the resources in the Selection Window. The RSSI value is averaged over all the previous $t_R-100 \cdot j$ sub-frames ($j \in \mathbb{N}$, $1 \leq j \leq 10$) for $\lambda=10\text{Hz}$ ³ (Fig. 1). Vehicle v_i then randomly chooses one of the candidate resources in L_C , and reserves it for the next Reselection Counter transmissions.

III. TRANSMISSION ERRORS IN C-V2X MODE 4

C-V2X Mode 4 transmissions can encounter the following four mutually exclusive errors that are analytically quantified in the next section:

1) Errors due to half-duplex transmissions (*HD*). The C-V2X radio is half-duplex. This error is then produced when a

¹ p_{res} is usually set equal to 0 and does not have a strong impact on the process [13]. This value is also assumed in this study.

² For $\lambda=20\text{Hz}$, $j=i-50 \cdot k$ and $k \in \mathbb{N}$, $1 \leq k \leq 20$. For $\lambda=50\text{Hz}$, $j=i-20 \cdot k$ and $k \in \mathbb{N}$, $1 \leq k \leq 50$.

³ For $\lambda=20\text{Hz}$, $t_R-50 \cdot j$ sub-frames ($j \in \mathbb{N}$, $1 \leq j \leq 20$). For $\lambda=50\text{Hz}$, $t_R-20 \cdot j$ sub-frames ($j \in \mathbb{N}$, $1 \leq j \leq 50$).

packet cannot be received by a vehicle because it is transmitting its own packet in the same sub-frame. This type of error does not depend on the distance between transmitter and receiver, but just on the probability that two vehicles select the same sub-frame to transmit their packets. The probability of not correctly receiving a packet due to this effect is here referred to as δ_{HD} :

$$\delta_{HD} = \Pr(e = HD) \quad (1)$$

- 2) Error due to a received signal power below the sensing power threshold (SEN). This error is produced when a packet is received with a signal power below the sensing power threshold P_{SEN} , and hence it cannot be decoded. This error mainly depends on the transmission power, the sensing power threshold, the propagation and the distance between transmitter and receiver. This type of error excludes those quantified in 1). The probability of not correctly receiving a packet due to this effect is here referred to as δ_{SEN} :

$$\delta_{SEN} = \Pr(e = SEN | e \neq HD) \quad (2)$$

- 3) Error due to propagation effects. In this case, a packet is received with a signal power higher than P_{SEN} but the received SNR (Signal to Noise Ratio) is not sufficient to guarantee the correct reception of the packet. This type of error does not consider interferences and collisions (i.e. it is only due to propagation effects), and hence depends on the same factors as 2) plus also on the MCS. In this study, this type of error excludes those quantified in 1) and 2). The probability of not correctly receiving a packet due to this effect is here referred to as δ_{PRO} :

$$\delta_{PRO} = \Pr(e = PRO | e \neq HD, e \neq SEN) \quad (3)$$

- 4) Error due to packet collisions (COL). This error is produced when a vehicle transmits on the same resource (i.e. the same sub-channel and sub-frame) than another vehicle, and the interference generated prevents the correct reception of the packet by the receiver due to insufficient SINR (Signal to Interference and Noise Ratio). In this study, this type of error excludes those quantified in 1), 2) and 3). The probability of not correctly receiving a packet due to this effect is referred to as δ_{COL} :

$$\delta_{COL} = \Pr(e = COL | e \neq HD, e \neq SEN, e \neq PRO) \quad (4)$$

IV. ANALYTICAL MODELS

This section analytically quantifies the four possible transmission errors in C-V2X Mode 4, and presents an analytical model of the PDR as a function of the distance between transmitter and receiver. To this aim, we consider a highway scenario with multiple lanes. Given the ratio between the length and width of a highway, we assume that this scenario is equivalent to a single-lane scenario where vehicles are separated by $1/\beta$ meters (i.e. a traffic density of β vehicles per meter). All vehicles periodically transmit λ packets per second on the same 10MHz channel with transmission power P_t . We consider that all packets have the same size (B bytes)

and are transmitted using the same MCS.

To derive the analytical expressions, we consider that vehicle v_t will act as transmitter, and vehicle v_r as receiver. Both vehicles are separated by a distance d . The distance between transmitter and receiver affects most of the types of errors identified since it influences the received signal power and the probability of packet collision. The analytical models proposed consider that a packet is correctly received if none of the identified types of error occur. Since these errors are exclusive, the PDR can be calculated as:

$$PDR = (1 - \delta_{HD}) \cdot (1 - \delta_{SEN}) \cdot (1 - \delta_{PRO}) \cdot (1 - \delta_{COL}) \quad (5)$$

We can normalize the probability of each type of error, and express the PDR as:

$$PDR = 1 - \hat{\delta}_{HD} - \hat{\delta}_{SEN} - \hat{\delta}_{PRO} - \hat{\delta}_{COL} \quad (6)$$

where

$$\hat{\delta}_{HD} = \delta_{HD} \quad (7)$$

$$\hat{\delta}_{SEN} = (1 - \delta_{HD}) \cdot \delta_{SEN} \quad (8)$$

$$\hat{\delta}_{PRO} = (1 - \delta_{HD}) \cdot (1 - \delta_{SEN}) \cdot \delta_{PRO} \quad (9)$$

$$\hat{\delta}_{COL} = (1 - \delta_{HD}) \cdot (1 - \delta_{SEN}) \cdot (1 - \delta_{PRO}) \cdot \delta_{COL} \quad (10)$$

$$0 \leq \delta_{HD}, \delta_{SEN}, \delta_{PRO}, \delta_{COL} \leq 1 \quad (11)$$

$$0 \leq \hat{\delta}_{HD} + \hat{\delta}_{SEN} + \hat{\delta}_{PRO} + \hat{\delta}_{COL} \leq 1 \quad (12)$$

A. Half-duplex errors

The probability that two vehicles cannot receive their packets because of the half-duplex effect does not depend on their distance, the C-V2X Mode 4 SPS scheme, or the channel occupancy. Two vehicles have certain probability of selecting the same sub-frame for transmitting their packets. This probability depends on the number of packets transmitted per vehicle per second, and the number of sub-frames within a second. Considering 1ms sub-frames, the probability of not receiving a packet due to the half-duplex effect can be approximated by the following equation:

$$\delta_{HD} = \frac{\lambda}{1000} \quad (13)$$

This effect is local and only affects those vehicles transmitting in the same sub-frame, i.e. vehicles transmitting in other sub-frames can still receive the packets.

B. Errors due to a received signal power below the sensing power threshold

To calculate the probability of receiving a packet with a signal power below the sensing power threshold, we take into account the pathloss (PL) and shadowing (SH). The pathloss represents the average signal attenuation with the distance between transmitter and receiver, and is typically modeled with a log-distance function. The shadowing represents the effects of obstacles on the signal attenuation, and is modeled with a log-normal random distribution with zero mean and variance σ . The received signal power P_r at the receiver is

therefore a random variable that can be expressed as:

$$P_r = P_t - PL - SH \quad (14)$$

where P_t is the transmission power, PL is the pathloss at the distance d , and all variables are in dB. The probability that the received signal power is lower than the sensing power threshold P_{SEN} is:

$$\delta_{SEN} = \int_{-\infty}^{P_{SEN}} PDF(P_r) dP_r \quad (15)$$

The shadowing follows a log-normal random distribution, so the PDF of the received signal power can be expressed as:

$$PDF(P_r) = \frac{1}{\sigma\sqrt{2\pi}} \exp\left(-\left(\frac{P_t - PL - P_r}{\sigma\sqrt{2}}\right)^2\right) \quad (16)$$

The combination of equations (15) and (16) results in that the probability that the received signal power at d is lower than the sensing power threshold is equal to:

$$\delta_{SEN} = \frac{1}{2} \left(1 - \text{erf}\left(\frac{P_t - PL - P_{SEN}}{\sigma\sqrt{2}}\right)\right) \quad (17)$$

where erf is the well-known error function.

$1 - \delta_{SEN}$ is the PSR (Packet Sensing Ratio), and eq. (17) can be generalized to compute PSR at any distance d :

$$PSR(d) = \frac{1}{2} \left(1 + \text{erf}\left(\frac{P_t - PL - P_{SEN}}{\sigma\sqrt{2}}\right)\right) \quad (18)$$

C. Error due to propagation

The probability that a packet is lost due to propagation effects depends on the PHY layer performance of the receiver. This performance is modeled in this study using link level Look-Up Tables reported in [14]. These LUTs provide the Block Error Rate (BLER) as a function of the SNR for a given packet size, MCS, propagation environment and relative speed between transmitter and receiver. To model transmission errors due to propagation effects, we consider that the SNR at a receiver is a random variable expressed in dB as:

$$SNR = P_r - N_0 = P_t - PL - SH - N_0 \quad (19)$$

where N_0 is the noise power. At a given distance between transmitter and receiver, PL is constant, and therefore SNR follows the same random distribution as SH but with a mean value equal to $P_t - PL - N_0$. The probability that a packet is lost due to propagation effects can hence be expressed as:

$$\delta_{PRO} = \sum_{SNR=-\infty}^{+\infty} BLER(SNR) \cdot PDF_{P_r > P_{SEN}}(SNR) \quad (20)$$

where

$$PDF_{P_r > P_{SEN}}(SNR) = \begin{cases} \frac{PDF(SNR)}{1 - \delta_{SEN}} & \text{if } P_r > P_{SEN} \\ 0 & \text{if } P_r \leq P_{SEN} \end{cases} \quad (21)$$

In eq. (20), the term $BLER(SNR)$ represents the BLER for certain SNR following the LUTs in [14]. This term is multiplied by the PDF of the SNR for those SNR values for

which the P_r is higher than P_{SEN} . The objective is to omit those packets with a received signal power lower than the sensing power threshold P_{SEN} ; these packets have been already taken into account in δ_{SEN} (eq. (15)). The PDF(SNR) needs to be normalized by $1 - \delta_{SEN}$ in eq. (21) so that the integral of this equation between $-\infty$ and $+\infty$ is 1, and the probability δ_{PRO} of not receiving a packet due to propagation effects is a value between 0 and 1.

D. Errors due to packet collisions

This error is produced when a given interfering vehicle (v_i) transmits on the same sub-frame and sub-channel than the transmitting vehicle (v_t), and the interference generated prevents the correct reception of the packet by the receiver (v_r). To estimate the probability of losing a packet due to this type of error, it is necessary to calculate: 1) the probability $p_{COL}(v_i)$ that a packet collision occurs between the transmitter v_t and vehicle v_i , and 2) the probability $p_{INT}(v_i)$ that the interference generated by v_i on the receiver v_r provokes that the packet transmitted by v_t cannot be correctly received at v_r . The probability of packet loss due to a collision provoked by vehicle v_i can therefore be expressed as:

$$\delta_{COL}^i = p_{COL}(v_i) \cdot p_{INT}(v_i) \quad (22)$$

$p_{COL}(v_i)$ depends on the sensing-based SPS scheme defined in C-V2X Mode 4. On the other hand, $p_{INT}(v_i)$ depends on the propagation conditions and the distances between vehicles v_r , v_t and v_i . The probability of packet loss due to a collision provoked by any vehicle in the scenario can be derived from equation (22) as:

$$\delta_{COL} = 1 - \prod_i (1 - \delta_{COL}^i) \quad (23)$$

To calculate $p_{INT}(v_i)$ we assume that the negative effect of the interference received from vehicle v_i over the received signal is equivalent to additional noise. The SINR experienced by the receiver can be expressed as:

$$SINR = P_r - (P_i + N_0) \quad (24)$$

where all variables are in dB or dBm, and P_i is the signal power received from the interfering vehicle v_i . $SINR$ is therefore a random variable that results from the addition of two random variables (P_r and P_i). The PDF of the $SINR$ can hence be obtained from the cross correlation of the PDF of the P_r and P_i variables [15]. As a result, the probability that the receiver receives a packet with error due to low $SINR$ (i.e. low P_r and/or high P_i) can be computed as:

$$p_{SINR}(v_i) = \sum_{SINR=-\infty}^{+\infty} BLER(SINR) \cdot PDF_{P_r > P_{SEN}}(SINR) \quad (25)$$

This equation includes the packets that could not be received due to propagation effects, i.e. those packets that would have been lost even without the interference received from v_i . Since these packets were already considered in δ_{PRO} , we need to perform the following normalization to only consider those packets that are lost due to collisions in p_{INT} :

$$p_{INT}(v_i) = \frac{p_{SINR}(v_i) - \delta_{PRO}}{1 - \delta_{PRO}} \quad (26)$$

where δ_{PRO} is obtained from eq. (20). The same LUTs used to calculate δ_{PRO} in equation (20) (and obtained from [14]) can be used in equation (25) to estimate $BLER(SINR)$ assuming that the negative effect of the interference over the received signal is equivalent to additional noise.

$p_{COL}(v_i)$ represents the probability that the transmitting vehicle v_i and an interfering vehicle v_i transmit in the same sub-channel and the same sub-frame. To calculate this probability, we need the following definitions (see Fig. 2): N is the total number of resources in all sub-frames contained in the Selection Window; N_E is the number of resources excluded in Step 2 of the sensing-based SPS scheme of C-V2X Mode 4; N_A is the number of assignable resources, i.e. those resources that were not excluded by Step 2 (i.e. N_A is equal to the size of list L_A , and $N_A = N - N_E$); N_C is the number of candidate resources that could be used by the transmitting vehicle after Steps 2 and 3, and is therefore equal to the size of list L_C . N_C is equal to the 20% of N [1]. Given that the traffic density is constant, and that vehicles are uniformly distributed in the scenario and have the same transmission parameters, we assume that all vehicles have the same N , N_E , N_A and N_C .

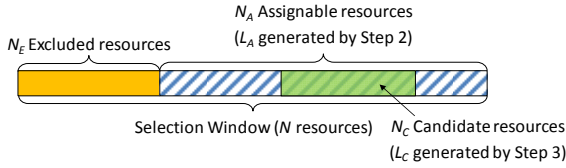


Fig. 2. Classification of resources following the sensing-based SPS scheme.

To reduce the complexity of the analytical model, we separate the derivation of $p_{COL}(v_i)$ under Steps 2 and 3 of the sensing-based SPS scheme. This approach is motivated by the fact that it is not always necessary to take into account both Steps as it is next explained:

Step 3 has limited effect on the resource selection process when the channel load is high. This is the case because when the channel load is high, Step 2 excludes most of the resources, and the size of the list of available resources L_A is equal to the 20% of all resources in the Selection Window. Step 3 builds the list of candidate resources L_C from list L_A . The size of L_C must be equal to the 20% of all resources in the Selection Window. So when the channel load is high, Step 3 would not modify the resources selected by Step 2 (Fig. 3a). As a result, when the channel load is high, $p_{COL}(v_i)$ is equal to the probability that a packet collision occurs when only Step 2 is executed:

$$p_{COL}(v_i) = p_{COL}^{[2]}(v_i) \quad (27)$$

Step 2 has limited effect on the resource selection process when the channel load is low. When the channel load is low, Step 2 would exclude only a few resources to build the list of available resources L_A . Step 3 would build the list of candidate resources L_C by selecting from L_A those resources with the lowest average RSSI over the last 1000 sub-frames. Step 3 is

able to exclude the resources that Step 2 would exclude, and the same L_C could be obtained even if Step 2 was not executed (Fig. 3b). The utility of Step 2 is hence limited under low channel load levels. As a result, when the channel load is low, $p_{COL}(v_i)$ is equal to the probability that a packet collision occurs when only Step 3 is executed:

$$p_{COL}(v_i) = p_{COL}^{[3]}(v_i) \quad (28)$$

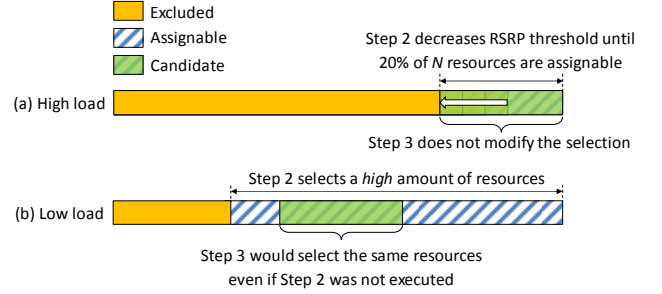


Fig. 3. Impact of Step 2 and Step 3 of sensing-based SPS on L_C for low and high channel load levels.

Step 2 and Step 3 need to be considered for intermediate channel load levels. Under intermediate channel load levels, we model the probability of packet collision $p_{COL}(v_i)$ as:

$$p_{COL}(v_i) = \alpha \cdot p_{COL}^{[2]}(v_i) + (1 - \alpha) \cdot p_{COL}^{[3]}(v_i) \quad (29)$$

where $\alpha \in [0, 1]$ is a weighting factor that represents the impact of Step 2 and Step 3 in the selection of the N_C candidate resources. If the channel load is high, $\alpha = 1$ because only Step 2 has an influence on the resources selected and Step 3 is not needed. If the channel load is low, $\alpha = 0$ because only Step 3 is needed. The specific value of α depends on the channel load, which is measured in this study using the CBR (Channel Busy Ratio) that represents the average number of resources sensed as busy. The C-V2X Mode 4 simulator described in Section V has been utilized to derive α through simulation. To this aim, $p_{COL}(v_i)$, $p_{COL}^{[2]}(v_i)$ and $p_{COL}^{[3]}(v_i)$ have obtained through simulation, and their values have been used to calculate α as a function of the CBR (depicted in Fig. 4 as dots). The value of α has been derived considering a wide range of transmission parameters and traffic densities. Fig. 4 also represents the linear approximation of α that is used in our analytical model:

$$\alpha = \begin{cases} 0 & \text{if } CBR < 0.2 \\ 2 \cdot CBR - 0.4 & \text{if } 0.2 \leq CBR \leq 0.7 \\ 1 & \text{if } CBR > 0.7 \end{cases} \quad (30)$$

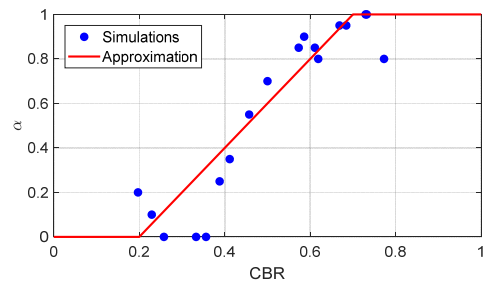


Fig. 4. Weighting factor α in equation (29).

To derive $p_{COL}(v_i)$, we derive first $p_{COL}^{[2]}(v_i)$ and $p_{COL}^{[3]}(v_i)$, which represent the probability that a packet collision occurs between v_t and v_i when only Step 2 or Step 3 are executed, respectively. If only Step 2 was executed, each vehicle would create its set of candidate resources L_C by randomly selecting them from its set of assignable resources L_A (i.e. there is no Step 3 to select the resources with lowest RSSI). Each vehicle then randomly selects the resource that will be used to transmit a packet from the set of N_C candidate resources. As a result, the probability that two vehicles select the same resource for transmission depends on the number of candidate resources that they have in common. This number is here referred to as the number of overlapped candidate resources O_C . Since the N_C candidate resources are selected from the N_A assignable resources, O_C depends on the number of overlapped assignable resources O_A , i.e. on how many resources their respective L_A lists have in common. In turn, O_A depends on the number of overlapped excluded resources, O_E , which are those resources excluded by both vehicles. Fig. 5 conceptually illustrates the concept of overlapped candidate, assignable, and excluded resources for vehicles v_t and v_i .

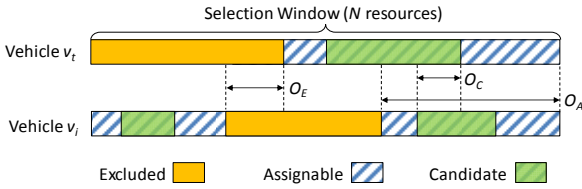


Fig. 5. Illustration of overlapped excluded (O_E), assignable (O_A) and candidate (O_C) resources for two vehicles.

$p_{COL}^{[2]}(v_i)$ depends on the number of overlapped candidate resources between vehicles v_t and v_i , O_C . It also depends on the probability $p_s(v_i)$ that v_t and v_i do not take into account their respective transmissions before selecting a new resource. This can occur if the two vehicles cannot sense each other, or when v_t and v_i select their resources nearly at the same time and hence they cannot take into account each other's selection as they have not been able yet to sense any packet transmitted using the newly selected resource. The probability that a packet collision occurs between the transmitter v_t and an interfering vehicle v_i during Step 2 of the sensing-based SPS scheme can then be expressed as:

$$p_{COL}^{[2]}(v_i) = p_s(v_i) \cdot \frac{O_C(v_i)}{N_C} \quad (31)$$

where $O_C(v_i)$ is the number of overlapped candidate resources between v_t and v_i . It is hence necessary to compute $p_s(v_i)$ and $O_C(v_i)$ to determine $p_{COL}^{[2]}(v_i)$. $p_s(v_i)$ depends on: 1) $PSR(d_i)$ (see eq. (18)) as it represents the probability that the transmitting and interfering vehicles (v_t and v_i , separated by a distance d_i) are able to sense their respective transmissions, and 2) the average number of consecutive packet transmissions τ for which each vehicle has used the same

resource⁴. $p_s(v_i)$, $PSR(d_i)$, and τ are related as follows:

$$p_s(v_i) = 1 - (1 - 1/\tau) \cdot PSR(d_i) \quad (32)$$

If the transmitting and interfering vehicles (v_t and v_i) are out of each other's sensing range (i.e. $PSR(d_i)=0$), they will not detect their respective transmissions and hence $p_s(v_i)=1$. When both vehicles are close to each other and $PSR(d_i)=1$, they will detect each other and can consider their previous transmissions in the resource selection process. This is however not possible if one of the two vehicles has to select a resource and the other vehicle has just selected its resource but has not yet made any transmission using the newly selected resource. This effect occurs with probability $1/\tau$, and therefore decreases as τ increases.

$O_C(v_i)$ is a function of the number of overlapped assignable resources $O_A(v_i)$. When Step 3 is not executed, $O_A(v_i)$ is equal to the number of assignable resources that both the transmitting vehicle v_t and the interfering vehicle v_i did not exclude in Step 2 of the sensing-based SPS algorithm. Since vehicles randomly select their resource from their set of assignable resources when Step 3 is not modeled, the relationship between $O_C(v_i)$, $O_A(v_i)$, the number of candidate resources N_C , and the number of assignable resources N_A can be expressed as:

$$\left(\frac{O_C(v_i)}{N_C} \right) \cdot N_A = \left(\frac{O_A(v_i)}{N_A} \right) \cdot N_C \quad (33)$$

and hence:

$$O_C(v_i) = O_A(v_i) \cdot \left(\frac{N_C}{N_A} \right)^2 \quad (34)$$

Using Fig. 5, it is possible to relate $O_A(v_i)$ and $O_E(v_i)$ as:

$$O_A(v_i) = N - 2 \cdot N_E + O_E(v_i) \quad (35)$$

N is the total number of resources in the Selection Window, and can be computed as follows considering that there are 1000 sub-frames per second:

$$N = 1000 \cdot \frac{S}{\lambda} \quad (36)$$

where S is the number of resources per sub-frame.

N_E depends on the traffic density, the total number of resources in the Selection Window, the transmission power and the propagation conditions, and is here estimated⁵ as:

$$N_E = \frac{S_{PSR}}{2} + \sum_{k=1}^{S_{PSR}/2} \max \left(1 - \frac{k}{N - S_{PSR}/2}, 0 \right) \quad (37)$$

where S_{PSR} represents the average number of vehicles that could be sensed if there were no packet collisions:

$$S_{PSR} = \sum_{i=-\infty}^{+\infty} PSR \left(\frac{i}{\beta} \right) = \beta \cdot \sum_{i=-\infty}^{+\infty} PSR(i) \quad (38)$$

⁴ For example, $\tau=(15+5)/2$ in the C-V2X Mode 4 when $\lambda=10$ Hz, since the Reselection Counter is randomly selected between 5 and 15.

⁵ This approximation has been validated through simulations using the C-V2X Mode 4 simulator presented in Section V.

where β is the traffic density in vehicles/m.

To calculate $O_E(v_i)$, let's consider that a vehicle v_k is transmitting in a given resource. The probability that two vehicles (v_i and v_j) exclude the resource used by vehicle v_k depends on their distance to v_k (d_{i-k} and d_{j-k} respectively), and is equal to $PSR(d_{i-k}) \cdot PSR(d_{j-k})$. In the considered scenario, this probability can also be expressed as $PSR(d_{i-k} + d_{j-k}) \cdot PSR(d_{i-k})$. If v_i and v_j are at the same location, they would exclude approximately the same resources because they would sense the transmissions of approximately the same vehicles. However, if vehicles v_i and v_j are separated by long distances, the resources excluded by each one of them can be considered independent. In this case, the proportion of overlapped excluded resources between both vehicles tends to N_E/N , and therefore the number of overlapped resources O_E tends to N_E^2/N . We can then compute O_E for vehicles v_i and v_j separated by a distance d_i as:

$$O_E(v_i) = \frac{R_{PSR}(d_i)}{R_0} \left(\frac{\beta \cdot N_E \cdot R_0}{S_{PSR}} - \frac{N_E^2}{N} \right) + \frac{N_E^2}{N} \quad (39)$$

where

$$R_0 = R_{PSR}(0) \quad (40)$$

and $R_{PSR}(d_i)$ is the autocorrelation of the PSR function at distance d_i :

$$R_{PSR}(d_i) = \sum_{j=-\infty}^{+\infty} PSR\left(\frac{j}{\beta} + d_i\right) \cdot PSR\left(\frac{j}{\beta}\right) \quad (41)$$

In eq. (41), please note that the distance between two consecutive vehicles is $1/\beta$ when the traffic density is β , and that is why the term j/β is introduced.

Combining equations (31)-(41), we can compute $p_{COL}^{[2]}(v_i)$ that represents the probability of packet collision between the transmitting vehicle v_i and an interfering vehicle v_j when only Step 2 of the sensing-based SPS scheme is considered.

To compute $p_{COL}^{[3]}(v_i)$, we follow a similar approach than for $p_{COL}^{[2]}(v_i)$. $p_{COL}^{[3]}(v_i)$ can be computed as:

$$p_{COL}^{[3]}(v_i) = p_s(v_i) \cdot \frac{O_C(v_i)}{N_C^2} \quad (42)$$

Since the relationship between O_C , O_A and O_E is maintained, equations (31) to (41) proposed for Step 2 are also used to compute $p_{COL}^{[3]}(v_i)$ when only Step 3 of the sensing-based SPS scheme is considered, except for equation (37) that is used to calculate N_E . To calculate N_E when only Step 3 is executed, we have to consider that L_C is built from the assignable resources, and Step 3 excludes those resources with the highest RSSI experienced during the last 1000 sub-frames. When the channel load is high, it is possible that Step 3 excludes more than 80% of the resources. Since the size of L_C must be $0.2 \cdot N$, if more than $0.8 \cdot N$ resources are excluded, Step 3 must consider as assignable certain resources that it had previously excluded until filling L_C . To this aim, Step 3 selects the resources with the lowest average RSSI. We model this process by virtually increasing the sensing power threshold

from P_{SEN} to certain $P_{SEN} + n \cdot \Delta$ where n is a positive integer and Δ is certain small increment in dB. We need to find the minimum value of n that reduces the number of excluded resources to less than $0.8 \cdot N$, and hence helps fill L_C . This is equivalent to finding the minimum value of n that satisfies the following relation:

$$\frac{S_{PSR}^{(n)}}{2} + \sum_{k=1}^{S_{PSR}^{(n)}/2} \max\left(1 - \frac{k}{N - S_{PSR}^{(n)}/2}, 0\right) \leq 0.8 \cdot N \quad (43)$$

where

$$S_{PSR}^{(n)} = \sum_{i=-\infty}^{+\infty} PSR_n\left(\frac{i}{2\beta}\right) = 2\beta \cdot \sum_{i=-\infty}^{+\infty} PSR_n(i) \quad (44)$$

$$PSR_n(d) = \frac{1}{2} \left(1 + \operatorname{erf}\left(\frac{P_T - PL - (P_{SEN} + n \cdot \Delta)}{\sigma \sqrt{2}}\right) \right) \quad (45)$$

Eq. (44) considers a 2β factor instead of β as in eq. (38). This is the case because Step 3 takes into account the last 1000 sub-frames. In 1000 sub-frames, each vehicle transmits in 2 different resources on average (i.e. it will perform one resource re-selection per second on average). For example, for $\lambda=10\text{Hz}$, each vehicle performs a resource selection every $(5+15)/2=7.5$ packet transmissions on average, i.e. every 750 sub-frames or 750ms. To take this effect into account in Step 3, we have estimated S_{PSR} (i.e. the average number of vehicles that could be sensed if there were no packet collisions) considering that the traffic density β is double.

Given that the PSR_n function monotonically decreases as n increases, we can solve the problem by evaluating increasing values of n , starting at $n = 0$. Once the minimum value of n that satisfies equation (43) is found, the number of excluded resources that will not be part of L_C can be approximated as:

$$N_E = \frac{S_{PSR}^{(n)}}{2} + \sum_{k=1}^{S_{PSR}^{(n)}/2} \max\left(1 - \frac{k}{N - S_{PSR}^{(n)}/2}, 0\right) \quad (46)$$

Equations (31) to (40) proposed for Step 2 are then used to compute $p_{COL}^{[3]}(v_i)$ when only Step 3 of the sensing-based SPS scheme is considered. In this case, the number of excluded resources, N_E , is defined by eq. (46) and not eq. (37).

The probability of packet collision $p_{COL}(v_i)$ is then computed following eq. (29) that relates $p_{COL}^{[2]}(v_i)$ and $p_{COL}^{[3]}(v_i)$. The value of α is calculated using eq. (30) considering that the channel occupancy or CBR can be analytically estimated as:

$$CBR = \frac{N_E}{N} \quad (47)$$

where the number of excluded resources N_E is calculated with eq. (37) for Step 2 since it considers the last Selection Window (Step 3 considers the last 1000 sub-frames).

Finally, the PDR is computed using eq. (5) where δ_{HD} , δ_{SEN} , δ_{PRO} and δ_{COL} are obtained from eq. (13), (17), (20) and (23), respectively.

V. MODEL VALIDATION

A. Framework

The proposed C-V2X Mode 4 analytical models have been implemented in Matlab. The models are validated in this section by comparing their outcome with that obtained with a C-V2X Mode 4 simulator developed by the authors over Veins and presented in [9]. Veins integrates OMNET++ for wireless networking simulation with the open-source traffic simulation platform SUMO. The simulator was used in [2] to present a detailed analysis of the performance of C-V2X Mode 4. It implements the complete MAC of C-V2X Mode 4 including the sensing-based SPS scheme. The simulator implements the Winner+ B1 propagation model recommended by the European project METIS for D2D/V2V [16]. This model is valid for the frequency range 0.45-6GHz. The physical layer performance is modelled through the link level Look Up Tables presented in [14].

The accuracy of the proposed analytical models is estimated using the Mean Absolute Deviation (MAD) metric that quantifies the absolute difference between two vectors or curves of M elements, F_s and F_a :

$$MAD[\%] = \frac{100}{M} \sum_{i=1}^M |F_s(i) - F_a(i)| \quad (48)$$

The MAD metric is here used to compare the PDR (Packet Delivery Ratio) obtained through simulations and using the analytical model presented in this study. The metric is also used to estimate the accuracy of the analytical models proposed to compute the probability of experiencing each one of the four possible transmission errors in C-V2X Mode 4. Unless otherwise stated, the comparison is conducted considering that vehicles transmit packets at $\lambda=10\text{Hz}$ with a transmission power $P_T=20\text{dBm}$ and an MCS of QPSK 0.7. This setting results in that each packet occupies 10 RBs, and there are hence 4 sub-channels per sub-frame. However, the models have been validated for other transmission power levels, different packet transmission frequencies and an MCS of QPSK 0.5 (2 sub-channels per sub-frame). Table I summarizes the main traffic and communication parameters analyzed. The simulations have been executed considered a highway of 5km with 4 lanes (2 lanes per driving direction) and vehicles moving at 70km/h. To avoid boundary effects, statistics are only taken from the vehicles located in the 2km around the center of the simulation scenario.

TABLE I. PARAMETERS ANALYZED

Parameter	Description	Values analyzed
β	Traffic density	0.1, 0.2, 0.3 veh/m
P_T	Transmission power	20, 23
λ	Packet tx frequency	10, 20, 50 Hz
B	Packet size	190 bytes
S	Sub-channels per sub-frame	2 (QPSK 0.5) and 4 (QPSK 0.7)

B. Validation

Fig. 6 compares the PDR curves obtained with the proposed analytical model (dashed lines) and with the C-V2X Mode 4 simulator Veins (solid lines) for $P_T=20\text{dBm}$, $\lambda=10\text{Hz}$, 4 sub-channels per 1ms sub-frame, and different traffic densities. The figure clearly shows that the PDRs obtained with the

proposed analytical model closely match those obtained by simulation. This trend is maintained irrespective of the traffic density and the resulting CBR. For example, a traffic density β of 0.1veh/m resulted in an estimated CBR of approximately 0.23, while a traffic density of $\beta=0.3\text{veh/m}$ resulted in a CBR of 0.62 (CBR levels analytically estimated using eq. (47)). Fig. 6 shows that the analytical model is capable to provide an accurate PDR for low and high channel load levels. These results demonstrate the validity of the proposed analytical models under different channel loads and interference levels.

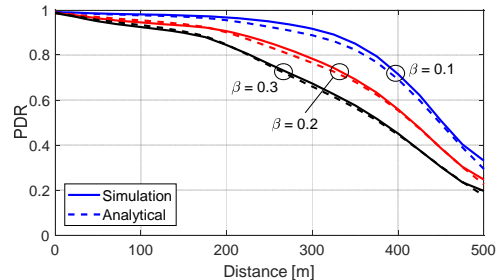


Fig. 6. PDR as a function of the distance between transmitter and receiver. $P_T=20\text{dBm}$, $\lambda=10\text{Hz}$, 4 sub-channels/sub-frame, and different traffic densities.

Fig. 7 depicts the probability of packet loss due to collisions ($\hat{\delta}_{COL}$ from eq. (7)) as a function of the distance between transmitter and receiver for $P_T=20\text{dBm}$, $\lambda=10\text{Hz}$, 4 sub-channels per 1ms sub-frame, and different traffic densities. Fig. 7 shows that the proposed analytical model is also capable to accurately quantify this type of packet errors as its performance closely matches that obtained through simulations. The same accuracy is observed for different traffic densities. Fig. 7 shows that the probability of losing a packet due to collisions has a maximum around 350-400m. This is the distance to the transmitter at which the hidden-node problem causes higher degradation in this scenario.

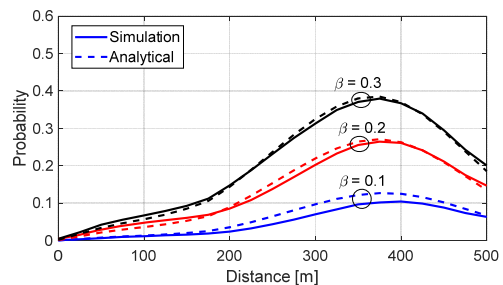


Fig. 7. Probability $\hat{\delta}_{COL}$ of packet loss due to collisions as a function of the distance between transmitter and receiver for $P_T=20\text{dBm}$, $\lambda=10\text{Hz}$, 4 sub-channels per 1ms sub-frame and different traffic densities.

Fig. 8 shows the probability of losing a packet due to the half-duplex effect ($\hat{\delta}_{HD}$ from eq. (8)), due to a received signal power below the sensing power threshold ($\hat{\delta}_{SEN}$ from eq. (9)) and due to the propagation ($\hat{\delta}_{PRO}$ from eq. (10)). The probabilities are shown as a function of the distance between transmitter and receiver for $P_T=20\text{dBm}$, $\lambda=10\text{Hz}$ and 4 sub-channels per 1ms sub-frame. These probabilities are independent of the traffic density. Fig. 8 shows again a good match in general between the values obtained by simulation and using the analytical models presented in this study. The probability of losing a packet due to the half-duplex effect

(Fig. 8a) depends on the duration of C-V2X sub-frames and the number of packets transmitted per second. However, it does not depend on the distance between transmitter and receiver or the traffic density. The probability of losing a packet due to propagation (Fig. 8a) is almost null at short distances, and has a maximum at around 450m to the transmitter. At higher distances, this probability decreases because most of the packets cannot even be detected due to a received signal power below the sensing power threshold. In fact, Fig. 8b depicts the probability of losing a packet because its received signal power is below the sensing power threshold. This probability increases as the distance to the transmitter increases.

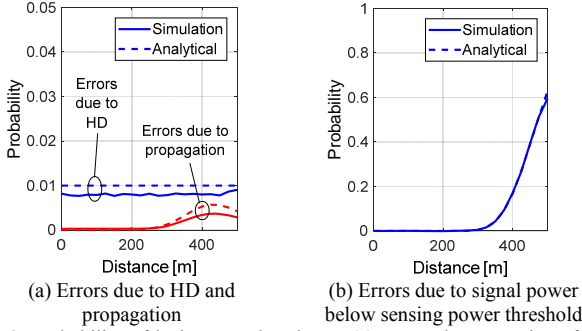


Fig. 8. Probability of losing a packet due to (a) HD and propagation effects, and due to a received signal power below the sensing power threshold (b). $P_t=20\text{dBm}$, $\lambda=10\text{Hz}$ and 4 sub-channels/sub-frame.

The proposed analytical models have also been evaluated for different transmission power levels. The transmission power level influences the received signal power and therefore the PDR. Fig. 6 depicted the PDR for $P_t=20\text{dBm}$, and Fig. 9 depicts it for $P_t=23\text{dBm}$. In this case, the analytical CBR ranged from 0.27 ($\beta=0.1\text{veh/m}$) to 0.69 ($\beta=0.3\text{veh/m}$). Fig. 9 shows again that the PDRs obtained with proposed analytical model closely match that obtained by simulation.

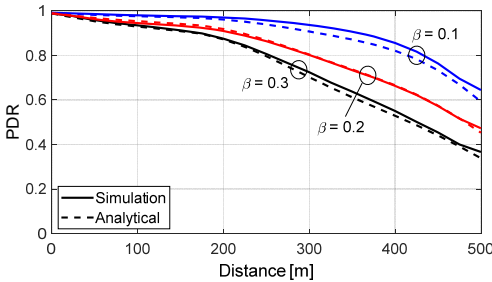


Fig. 9. PDR as a function of the distance between transmitter and receiver. $P_t=23\text{dBm}$, $\lambda=10\text{Hz}$, 4 sub-channels/sub-frame, and different traffic densities.

Another important parameter that influences the operation and performance of C-V2X Mode 4 is the number of packets transmitted per second per vehicle, λ . This parameter influences the number of sub-frames within the Selection Window, and the channel load and interference experienced by all vehicles. Fig. 10 shows the PDR obtained for $P_t=20\text{dBm}$ and $\lambda=20\text{Hz}$ for 3 traffic densities. The figure shows once more the close match between the PDRs obtained by simulation and using the proposed analytical models. For $\beta=0.3\text{veh/m}$, the channel load was so high (analytical CBR of 0.85) that the proposed model slightly deviates from the simulation results (6.5% mean absolute deviation). However,

it is important to consider that such high CBR levels would compromise the system's stability and scalability and should hence be avoided using congestion control mechanisms. In fact, relevant studies recommend that the target CBR for V2X systems using IEEE 802.11p should be in the range of 0.6-0.7 [17] and ETSI recommends a default maximum CBR of 0.5 [18]. The 3GPP has not defined yet a target CBR for C-V2X, but it is relevant highlighting that both IEEE 802.11p and C-V2X Mode 4 suffer from the hidden-terminal problem and hence from packet collisions.

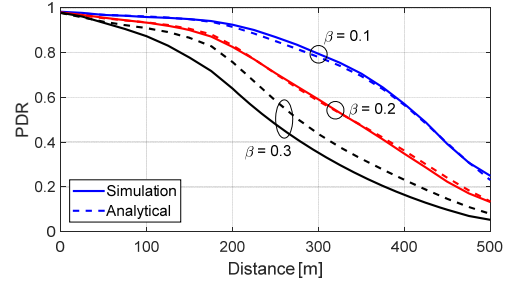


Fig. 10. PDR as a function of the distance between transmitter and receiver. $P_t=20\text{dBm}$, $\lambda=20\text{Hz}$, 4 sub-channels/sub-frame and different traffic densities.

The MCS influences the physical layer performance of C-V2X, the number of RBs that each packet occupies and hence the number of sub-channels per sub-frame. The previous results were obtained with a MCS of QPSK 0.7 (4 sub-channels per 1ms sub-frame). Fig. 11 shows the PDRs obtained with QPSK 0.5 (2 sub-channels per 1ms sub-frame). Fig. 11 demonstrates the validity of the presented analytical models for different MCS and number of sub-channels per sub-frame. The PDR is shown for traffic densities of 0.1, 0.2 and 0.3 veh/m that correspond to analytical CBR levels of 0.44, 0.74 and 0.86, respectively.

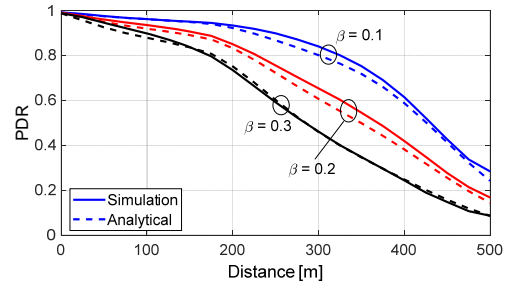


Fig. 11. PDR as a function of the distance between transmitter and receiver. $P_t=20\text{dBm}$, $\lambda=10\text{Hz}$, 2 sub-channels/sub-frame and different traffic densities.

The accuracy of the proposed analytical models is analyzed in Tables II, III and IV. These tables show the MAD of the PDR and the different types of transmission errors possible in C-V2X Mode 4 for different transmission power levels, traffic densities, packet transmission frequencies, and number of sub-channels per sub-frame (or MCS). The tables also show in the last column the CBR level (analytically estimated) for each combination of parameters reported in the tables. The results obtained show that the proposed model achieves a mean absolute deviation of the PDR smaller than 2.5% in all scenarios where the CBR is below 0.8. In many cases, the deviation is smaller than 1%, which demonstrates the high accuracy that can be achieved with the proposed analytical models. The tables show that the type of error that has a higher

contribution to the MAD of the PDF is actually the error due to packet collisions; this type of error was the most difficult to model due to the operation of C-V2X Mode 4 and its sensing-based SPS scheme.

TABLE II. MAD (MEAN ABSOLUTE DEVIATION) FOR THE PDR AND DIFFERENT TYPES OF ERRORS. $\lambda=10\text{Hz}$ AND 4 SUB-CHANNELS PER SUB-FRAME

P_T	β	PDR	HD	SEN	PRO	COL	CBR
20	0.1	1.60	0.19	0.21	0.07	1.25	0.23
	0.2	0.91	0.16	0.18	0.07	0.83	0.44
	0.3	0.92	0.14	0.20	0.07	0.84	0.62
23	0.1	1.95	0.21	0.14	0.05	1.59	0.27
	0.2	0.52	0.17	0.13	0.05	0.65	0.51
	0.3	1.24	0.18	0.15	0.05	0.94	0.69

TABLE III. MAD (MEAN ABSOLUTE DEVIATION) FOR THE PDR AND DIFFERENT TYPES OF ERRORS. $\lambda=20\text{Hz}$ AND 4 SUB-CHANNELS PER SUB-FRAME

P_T	β	PDR	HD	SEN	PRO	COL	CBR
20	0.1	0.74	0.36	0.18	0.07	0.55	0.44
	0.2	0.61	0.32	0.15	0.07	0.87	0.74
	0.3	6.28	0.25	0.19	0.07	6.63	0.86

TABLE IV. MAD (MEAN ABSOLUTE DEVIATION) FOR THE PDR AND DIFFERENT TYPES OF ERRORS. $\lambda=10\text{Hz}$ AND 2 SUB-CHANNELS PER SUB-FRAME

P_T	β	PDR	HD	SEN	PRO	COL	CBR
20	0.1	1.75	0.32	0.25	0.12	1.50	0.44
	0.2	2.50	0.27	0.18	0.12	2.28	0.74
	0.3	0.93	0.22	0.19	0.12	1.02	0.86

VI. CONCLUSIONS

This paper has presented the first analytical models of the communication performance of C-V2X or LTE-V Mode 4. In particular, the paper has presented models of the average PDR as a function of the distance between transmitter and receiver, and of the four types of transmission errors that can be encountered in C-V2X Mode 4 communications. The models are validated in this paper for a wide range of transmission parameters (transmission power, packet transmission frequency, and MCS) and traffic densities. To do so, the paper compares the results obtained with the analytical models to those obtained with a C-V2X Mode 4 simulator that has been developed by the authors over the Veins platform. The conducted analysis has shown that the analytical models are capable to accurately model the C-V2X Mode 4 communication performance. In fact, the mean absolute deviation of the results obtained with the analytical models is generally below 2.5% compared with the results obtained by simulation. The analytical models hence represent a valuable tool for the community to evaluate and provide insights into the communications performance of C-V2X Mode 4 under a wide range of parameters and conditions.

REFERENCES

- [1] 3GPP TS 36.300, "Evolved Universal Terrestrial Radio Access (E-UTRA) and Evolved Universal Terrestrial Radio Access Network (E-UTRAN); Overall description; Stage 2", Rel-14 V14.1.0, Dec. 2016.
- [2] R. Molina-Masegosa and J. Gozalvez, "LTE-V for Sidelink 5G V2X Vehicular Communications: A New 5G Technology for Short-Range Vehicle-to-Everything Communications", *IEEE Vehicular Technology Magazine*, vol. 12 (4), pp. 30-39, December 2017.
- [3] W. Min et al., "Comparison of LTE and DSRC-Based Connectivity for Intelligent Transportation Systems", *Proc. IEEE 85th Vehicular Technology Conference (VTC-Spring)*, Sydney (Australia), June 2017.
- [4] W. Li, X. Ma, J. Wu, K. S. Trivedi, X. L. Huang and Q. Liu, "Analytical Model and Performance Evaluation of Long-Term Evolution for Vehicle Safety Services", *IEEE Transactions on Vehicular Technology*, vol. 66, no. 3, pp. 1926-1939, March 2017.
- [5] A. Bazzi, B. M. Masini, A. Zanella and I. Thibault, "On the performance of IEEE 802.11p and LTE-V2V for the Cooperative Awareness of Connected Vehicles", *IEEE Transactions on Vehicular Technology*, vol. 66 (11), November 2017.
- [6] A. Bazzi, B. M. Masini and A. Zanella, "Performance Analysis of V2V Beaconing Using LTE in Direct Mode With Full Duplex Radios", *IEEE Wireless Communications Letters*, vol. 4, no. 6, pp. 685-688, Dec. 2015.
- [7] S. Fowler, C. H. Häll, D. Yuan, G. Baravdish and A. Mellouk, "Analysis of vehicular wireless channel communication via queueing theory model", *Proc. IEEE International Conference on Communications (ICC)*, Sydney (Australia), pp. 1736-1741, 2014.
- [8] A. Vinel, "3GPP LTE Versus IEEE 802.11p/WAVE: Which Technology is Able to Support Cooperative Vehicular Safety Applications?", *IEEE Wireless Communications Letters*, vol. 1, no. 2, pp. 125-128, April 2012.
- [9] R. Molina-Masegosa, J. Gozalvez, "System Level Evaluation of LTE-V2V Mode 4 Communications and its Distributed Scheduling", *Proc. IEEE 85th Vehicular Technology Conference (VTC-Spring)*, Sydney (Australia), 4-7 June 2017.
- [10] 3GPP TS 36.101, "Evolved Universal Terrestrial Radio Access (E-UTRA); User Equipment (UE) radio transmission and reception", Rel-14 V14.4.0, July 2017.
- [11] 3GPP TS 36.213, "Evolved Universal Terrestrial Radio Access (E-UTRA); Physical layer procedures", Rel-14 V14.3.0, June 2017.
- [12] 3GPP TS 36.321, "Evolved Universal Terrestrial Radio Access (E-UTRA); Medium Access Control (MAC) protocol specification", Rel-14 V14.3.0, June 2017.
- [13] A. Nabil, V. Marojevic, K. Kaur, C. Dietrich, "Performance Analysis of Sensing-Based SemiPersistent Scheduling in C-V2X Networks", *Proc. IEEE Vehicular Technology Conference Fall (VTC-Fall)*, Chicago (USA), 27-30 August 2018.
- [14] R1-160284, "DMRS enhancement of V2V," Huawei, HiSilicon, 3GPP TSG RAN WG1 Meeting #84, St Julian's, Malta, Feb. 2016.
- [15] G. Grimmett, D. Welsh, "Probability: An Introduction," *Oxford Science Publications*, ISBN-10: 0198709978, Nov. 2014.
- [16] METIS EU Project Consortium, "Initial channel models based on measurements", ICT-317669-METIS/D1.2, April 2014.
- [17] G. Bansal, J.B. Kenney, "Controlling Congestion in Safety-Message Transmissions: A Philosophy for Vehicular DSRC Systems", *IEEE Vehicular Technology Magazine*, vol. 8 (4), pp. 20-26, Dec. 2013.
- [18] ETSI TC ITS, "Intelligent Transport Systems (ITS); Decentralized Congestion Control Mechanisms for Intelligent Transport Systems operating in the 5 GHz range; Access layer part", TS 102 687 V1.1.1 July 2011.